Pressure-induced superconducting state of antiferromagnetic $CaFe_2As_2$

Hanoh Lee,[1] Eunsung Park,[2] Tuson Park,[1,2] V. A. Sidorov,[3] F. Ronning,[1] E. D. Bauer,[1] and J. D. Thompson[1]
[1]*Los Alamos National Laboratory, Los Alamos, New Mexico 87545, USA*
[2]*Department of Physics, Sungkyunkwan University, Suwon 440-746, Korea*
[3]*Vereshchagin Institute for High Pressure Physics, Troitsk 142190, Russia*
(Received 2 July 2009; published 31 July 2009)

The antiferromagnet $CaFe_2As_2$ does not become superconducting when subject to ideal hydrostatic pressure conditions, where crystallographic and magnetic states also are well defined. By measuring electrical resistivity and magnetic susceptibility under quasihydrostatic pressure, however, we find that a substantial volume fraction of the sample is superconducting in a narrow pressure range where collapsed tetragonal and orthorhombic structures coexist. At higher pressures, the collapsed tetragonal structure is stabilized with the boundary between this structure and the phase of coexisting structures strongly dependent on pressure history. Fluctuations in magnetic degrees of freedom in the phase of coexisting structures appear to be important for superconductivity.

DOI: 10.1103/PhysRevB.80.024519 PACS number(s): 74.62.Fj, 74.20.Mn, 74.25.Dw, 74.25.Fy

Discovery of superconductivity in the FeAs-layered compounds $RO_{1-x}F_xFeAs$ (R=La, Nd, Pr, Gd, and Sm) has attracted interest because of their high-superconducting transition temperatures, which appear to be well outside expectations of a conventional electron-phonon pairing mechanism.[1–6] Soon after reports of superconductivity in this "R1111" family of compounds,[1] another family of the Fe-As superconductors, AFe_2As_2 (A=Ca, Sr, Ba, and Eu), was discovered in which a nonmagnetic to antiferromagnetically ordered and tetragonal (T) to low-temperature orthorhombic (O) structural transition take place simultaneously above 100 K.[7–14] Superconductivity in the A122 family can be induced by electronic doping on the A and Fe sites[15,16] or by applied pressure.[17–19] Because of the relatively low pressures involved, the structural, magnetic, and superconducting transition temperatures in $CaFe_2As_2$ have been explored most extensively as a function of pressure.[17,18,20–23] These experiments led initially to conflicting conclusions about the temperature-pressure phase diagram of $CaFe_2As_2$. This controversy was resolved by realizing that slight nonhydrostatic conditions lead to superconductivity; whereas, measurements in a more hydrostatic environment provided by a liquid-helium pressure medium find no evidence for bulk superconductivity.[23] Under these conditions, phase boundaries delineating transitions from high-temperature tetragonal to low-temperature orthorhombic or collapsed tetragonal structures remain sharp and well-resolved as a function of pressure, in contrast to experiments with quasihydrostatic pressures. The higher pressures necessary to induce superconductivity in A=Sr and Ba prevent their study under ideal, hydrostatic conditions, with the result that their resistively determined pressure-temperature phase diagrams show substantial variability depending quasihydrostatic conditions.[19,24–28] Whether these compounds are similar to $CaFe_sAs_2$ in not supporting superconductivity under hydrostatic pressure remains unknown.

Though the observation of no superconductivity in $CaFe_2As_2$ under liquid-helium pressures is important for an interpretation of the physics of this material, the appearance of superconductivity with quasihydrostatic pressures also raises the interesting question of what is so different in these two cases. From measurements of the electrical resistivity, magnetic susceptibility, and strain as a function of pressure generated in a liquid pressure medium, we find that the temperature-pressure phase diagram of $CaFe_2As_2$ depends strongly on pressure history and that the superconducting volume fraction peaks in a narrow pressure range. As discussed below, these observations suggest that superconductivity emerges as a result of fluctuations associated with the complex state that appears in the pressure interval between approximately 0.3 and 0.8 GPa.

Platelike single crystals of $CaFe_2As_2$, which crystallize in the $ThCr_2Si_2$ tetragonal structure, were grown from a Sn flux.[12] Electrical resistivity measurements were performed using a conventional four-probe technique with an LR-700 resistance bridge, ac magnetic susceptibility measured at 157 Hz using a Stanford Lock-in Amplifier SR830, and strain determined from the resistance of a 12-μm-diameter constantan gauge glued along the tetragonal a axis. Resistivity and ac susceptibility of $CaFe_2As_2$ were measured simultaneously in a clamp-type Be-Cu pressure cell up to 1.52 GPa, where a silicone fluid was used to produce a quasihydrostatic pressure environment; whereas, strain measurements were performed separately but in the same pressure cell. The superconducting transition temperature of Pb was measured inductively to determine pressures at low temperature.[29] Independent studies show[30] that below 2 GPa the pressure gradient supported by silicone fluid is very low, provided it remains in the liquid state. Upon cooling, however, silicone fluid freezes into a structurally glassy state below a temperature $T_f \approx 122 + aP$, where a=87 K/GPa.[31] In the frozen state, the pressure gradient $\sigma \approx 0.07P$, so that at an average pressure of 1 GPa, the pressure gradient could be as large as 0.07 GPa.[30] By using samples that fill only a small fraction of the cell volume, we expect a smaller pressure gradient across the sample. Indeed, the maximum transition width of the Pb superconducting transition corresponded to about 0.01 GPa at the highest average pressure, signaling the presence of a small ($\leq 1\%$) pressure inhomogeneity.

Several single crystals were studied by electrical resistivity at ambient pressure; crystals with Sn inclusions showed

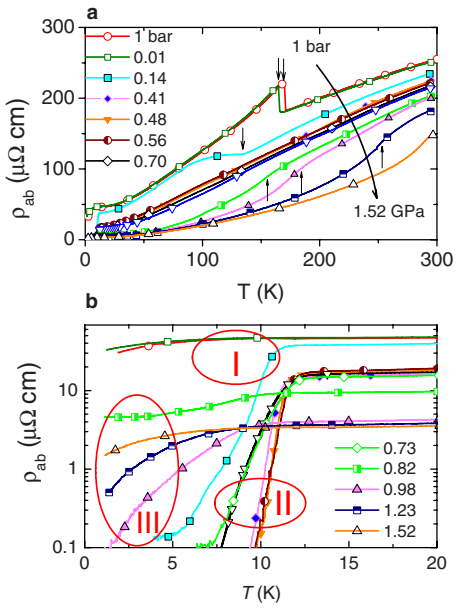

FIG. 1. (Color online) Electrical resistivity of $CaFe_2As_2$ under pressure. Curves were obtained on cooling, except for $P=1$ bar where measurements were made on both cooling and warming. The legends apply to both (a) and (b) and give the pressure in GPa. (a) In-plane resistivity ρ_{ab} from 1.2 to 300 K for pressures of 1 bar, 0.01, 0.14, 0.41, 0.48, 0.56, 0.7, 0.73, 0.82, 0.98, 1.23, and 1.52 GPa. Arrows denote temperatures for a phase change, as discussed in the text. For clarity, only one out of 50 data points is shown. (b) An expanded view of the low-temperature, in-plane resistivity ρ_{ab} shows the evolution of the superconducting transition temperature T_c. Sharp transitions appear only in a phase of coexisting O and cT structures. Curves corresponding to pressure regimes in Fig. 2(b) are circled. For clarity, one out of ten data points is shown.

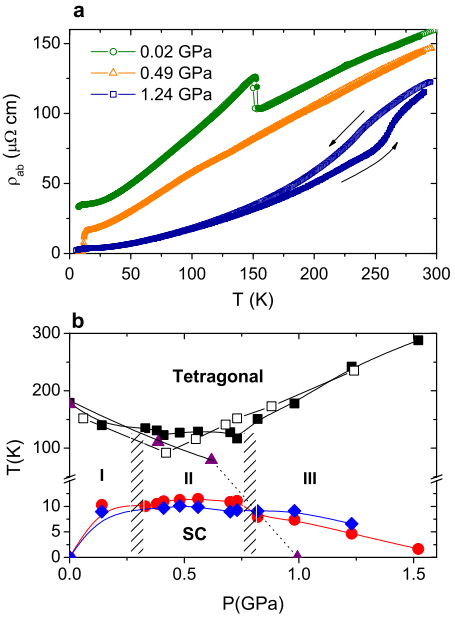

FIG. 2. (Color online) (a) Temperature-dependent resistivity upon cooling and warming in representative pressure ranges, corresponding to those in phases I, II, and III in (b). Note the emergence of strong thermal hysteresis at T_S^h in phase III. (b) Temperature-pressure phase diagram. Solid squares (increasing pressure) denote the structural transition temperature T_S from a tetragonal to a orthorhombic for $P<0.3$ GPa (phase I), a phase of coexisting O and cT structures for $0.3<P<0.8$ GPa (phase II), and the cT structure (phase III) for $P>0.8$ GPa. Open squares represent structural transitions determined with decreasing pressure. The transition temperatures were defined from a break or maximum in the slope of $d\rho/dT$. Hashed vertical lines separate these structural phases. Circles denote the midpoint of the resistive SC transition and diamonds the onset of superconductivity in ac magnetic susceptibility χ_{ac}. Triangles describe the magnetic transition from a paramagnetic to a SDW phase deduced from μSR measurements (Ref. 22).

a larger relative resistivity ratio [RRR$=\rho(300\ \mathrm{K})/\rho(0\ \mathrm{K})\sim 15$] and those without Sn inclusions had a smaller RRR ($\sim$5). When both types of samples were subject to pressure, however, characteristic features, such as the structural/antiferromagnetic transition temperature T_S and superconducting transition temperature T_c, were similar to each other. Below, we report data on single crystals $CaFe_2As_2$ free of Sn inclusions. Though the ambient-pressure RRR ($\sim$5) was small, it increased to greater than 50 at high pressure, indicating intrinsically high crystallinity with few defects.

Figure 1(a) displays the electrical resistivity (ρ_{ab}) of $CaFe_2As_2$ for electrical current flowing in the Fe-As plane. At ambient pressure, there is a steplike, hysteretic increase in the resistivity at 171 K($=T_S$), where the antiferromagnetic (AFM) and lattice-structural transitions coincide.[32] When cooled through T_S, the high-temperature tetragonal structure switches to an orthorhombic structure and the Fe spin is aligned along the orthorhombic a axis with an ordered moment 0.8 μ_B/Fe.[20] Pressure strongly suppresses T_S at an initial rate of -220 K/GPa and the transition width broadens. For pressures higher than 0.35 GPa, where neutron-diffraction measurements found a collapsed tetragonal (cT) structure at 0.63 GPa and 50 K,[21] a signature for T_S is hardly visible in the resistivity. In this higher pressure range, muon-spin resonance studies show that magnetic order persists to at least 0.62 GPa.[22] On the basis of symmetry, magnetic order with the ambient-pressure propagation wave vector must be associated with the O structure. With further increasing pressure ($P>0.75$ GPa), a break in the slope of the resistivity [marked by arrows in Fig. 1(a)] appears, and its temperature T_S^h increases with increasing pressure, which signals a change to essentially phase-pure cT structure.[23] (We note that experiments using a liquid-helium pressure medium find the low-temperature O-cT boundary at $P\approx 0.35$ GPa.[23]) As shown in Fig. 2(a), the transition at T_S^h is strongly hysteretic with temperature, and though not apparent in these figures, the RRR jumps from $\sim$15 to over 50 upon entering the new structural phase.

A slight downturn in the resistivity ρ_{ab} of $CaFe_2As_2$ is observed below 8 K at ambient pressure [Fig. 1(b)], possibly due to disconnected superconducting filaments. At a pressure of 0.14 GPa, the resistance drops by a factor of 300 at 5.4 K from its value at the superconducting (SC) onset temperature (=11.5 K). With further applied pressure, the resistive transition becomes sharp in a narrow pressure range, and the midpoint temperature T_c increases, goes through a maximum near 0.5 GPa and forms a wide pressure dome of T_c's [circles in Fig. 2(b)], consistent with an earlier report from experi-

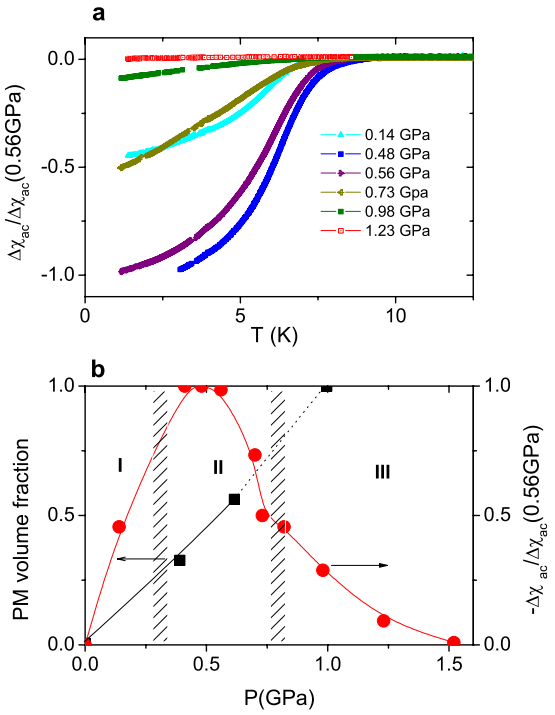

FIG. 3. (Color online) (a) Pressure evolution of normalized ac magnetic susceptibility $\Delta\chi_{ac}/\Delta\chi_{ac}$(=0.56 GPa) on a single crystal sample, where $\Delta\chi_{ac}=\chi_{ac}-\chi_{ac}(T_c)$. In these units, 1.0 corresponds to at least $0.5(1/4\pi)$ as explained in the text. The amplitude of the ac magnetic field was approximately 1 Oe. (b) Diamagnetic response $-\Delta\chi_{ac}(P)/\Delta\chi_{ac}$(0.56 GPa) (circles) at 1.2 K and volume fraction of a paramagnetic phase estimated by μSR measurements (squares), where the dotted line is an extrapolation (Ref. 22). Hashed vertical lines are the same as those shown in Fig. 2(b).

ments with quasihydrostatic pressure.[18] The existence of superconductivity over a wide pressure range suggests that a specific crystal structure is not a requirement for superconductivity in $CaFe_2As_2$, but as will be discussed, this conclusion is not supported by other measurements.

Squares in Fig. 2(b) denote transitions indicated by arrows in Fig. 1(a); whereas, triangles in Fig. 2(b) represent the AFM transition (T_N) obtained from μSR measurements.[22] Below 0.3 GPa, both T_N and T_S are suppressed at a similar rate under pressure. For pressures higher than 0.3 GPa, where a collapsed tetragonal structure grows in, the two transitions are decoupled: T_S is almost independent of pressure but T_N drops rapidly to zero kelvin between 0.62 and 1.0 GPa. The $T-P$ phase diagram in Fig. 2(b) shows the coexistence of magnetism and superconductivity.

The bulk nature of SC was investigated by ac magnetic susceptibility measurements, with results plotted in Fig. 3(a) for a single crystal sample. At a pressure close to 1 bar, there is no noticeable change in χ_{ac} (not shown) at low temperatures, which is consistent with other bulk measurements. With pressure, a drop in χ_{ac} occurs at the resistive midpoint T_c. The drop, reflecting the volume shielding fraction of superconductivity, initially increases with pressure, goes through a maximum between 0.4 and 0.6 GPa, and becomes negligible at 1.52 GPa [see Fig. 3(b)]. The change in χ_{ac} of $CaFe_2As_2$ at 0.5 GPa is at least 50% of perfect diamagnetism based on measurements in the same coil with known superconductors of similar shape and mass, ruling out filamentary superconductivity for $CaFe_2As_2$ in this pressure range. A similar diamagnetic response has been reported in superconducting crystals of $CaFe_{1.94}Co_{0.06}As_2$.[33]

Because these low-field ($\approx$1 Oe) ac susceptibility measurements reflect diamagnetic shielding of the bulk single crystal, these measurements were repeated on crushed crystals that were annealed for 24 h at 300 °C after crushing to remove potential strain induced by grinding them into powder. Scanning electron microscopy showed that the crushed powder was composed of thin (1–2 μm-thick) platelets but with a distribution of diameters (none larger than 100 μm in diameter with about 15% of the particles being in each of the ranges 50–80, 30–50, 10–30, and 5–10 μm and the remaining $\approx$40% having diameters of 1–5 μm). Susceptibility measurements on this powder gave the same evolution with pressure and nearly the same diamagnetic response that are shown in Fig. 3(a). The superconducting penetration depth in $CaFe_2As_2$ is not known but is $\approx$0.45 μm in $Ba_{0.55}K_{0.45}Fe_2As_2$ (Ref. 34) with $T_c=30$ K and close to this value in F-doped LaFeAsO ($T_c=18$ K).[35] With T_c in $CaFe_2As_2$ roughly half that in these other iron arsenide superconductors, we assume its penetration depth is roughly $\sqrt{2}$ larger, i.e., $\approx$0.6 μm.[34,36] Consequently, the ac magnetic field samples of order 60–100 % of the thickness of the crushed crystals and a comparable volume of the large fraction of smallest crystallites. Though still not completely a probe of superconductivity in the bulk, these experiments show that a substantial volume of $CaFe_2As_2$ supports superconductivity.

Squares in Fig. 3(b) represent the pressure evolution of the paramagnetic volume fraction (the fraction that is not ordered antiferromagnetically) of $CaFe_2As_2$ estimated independently from μSR measurements.[22] Neutron-diffraction[37] and NMR measurements[38] are consistent with this estimate being an upper limit on the paramagnetic volume fraction. At 0.4 GPa, the fractional diamagnetic response exceeds the paramagnetic volume fraction of the cT phase, indicating that the pressure-induced superconductivity in $CaFe_2As_2$ is not from a pure, phase-separated paramagnetic phase, but involves more of the sample volume.

Squares in Fig. 4(a) show the pressure evolution of the residual resistivity (ρ_0) of $CaFe_2As_2$, which was obtained from a least-squares fit of the low-temperature resistivity to a simple power law, $\rho=\rho_0+AT^n$. Values of $n(P)$ range between 2 and 3 (not shown) but ρ_0 is relatively insensitive to the precise value of n. The residual resistivity displays a sharp change at 0.3 and 0.8 GPa, where O to coexisting O/cT and O/cT to cT structure changes occur, respectively. In the orthorhombic ($P<0.3$ GPa) and collapsed tetragonal phase ($P>0.8$ GPa), ρ_0 monotonically decreases, but the residual resistivity and T_c are nonmonotonic, forming a dome around 0.56 GPa in the coexisting phase $0.3<P<0.8$ GPa, where the diamagnetic response is a maximum. The deviation from a monotonic decrease in ρ_0 signifies an additional scattering mechanism at low temperatures.

The existence of structural and magnetic inhomogeneity in phase II is central to the emergence of bulk superconductivity. NMR spectra obtained on $CaFe_2As_2$ under quasihydro-

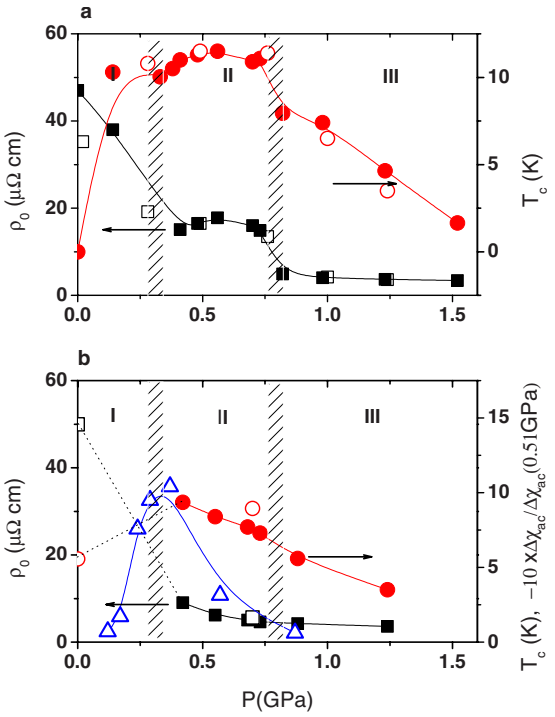

FIG. 4. (Color online) (a) Pressure dependence of the residual resistivity ρ_0 (squares) of $CaFe_2As_2$ plotted on the left ordinate and superconducting transition temperature T_c (circles) plotted on the right ordinate. Solid and open symbols are data obtained with increasing pressure, for the same crystal (1) reported in previous figures and for a second crystal (2), respectively. The residual resistivity of (2) was normalized to that of (1) at 1.2 GPa. Hashed vertical lines are the same as those shown in previous figures. (b) Residual resistivity and resistive midpoint T_c of crystal (1) (solid symbols) and for (2) (open symbols) obtained on decreasing pressure from 1.52 GPa. Open triangles are the normalized diamagnetic response, defined in Fig. 3, for decreasing pressure. Hashed lines from (a) are shown for comparison.

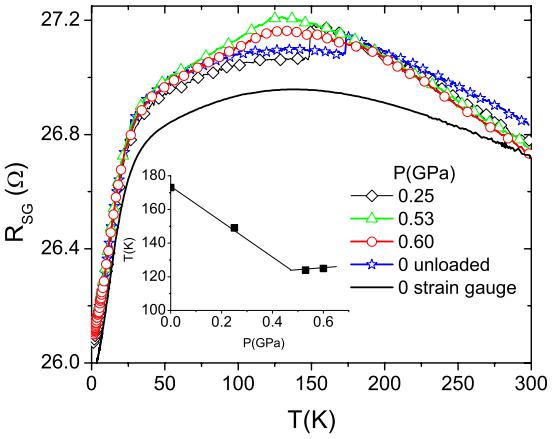

FIG. 5. (Color online) Temperature-dependent resistance of a constantan strain gauge glued along the tetragonal a axis of $CaFe_2As_2$. One of nine data points is shown for clarity. The change in resistance is proportional to strain, as discussed in the text. For comparison, the solid line is plot of the temperature-dependent resistance of the free-standing strain gauge at $P=0$. Measurements are plotted for various increasing pressures, except for the $P=0$ data that were obtained on decreasing pressure from 0.6 GPa. Note the sharp jump in resistance at the structural transition for $P=0$ and 0.25 GPa but only a broad peak for pressures corresponding to range II in Fig. 2(b). The inset is a plot of the structural transition temperature determined by these measurements, which are in good agreement with transition temperatures from resistivity measurements.

static pressure clearly reflect this inhomogeneity[38] as do stain-gauge measurements shown in Fig. 5. For pressures corresponding to phase I in Fig. 2(b), the strain gauge shows a sharp change in resistance at the structural/magnetic transition temperature. In this pressure range, the pressure medium remains a liquid to just below the structural transition temperature T_S. The value of this resistance change at T_S $\Delta R/R$ corresponds to a length change $\Delta L/L=-0.24\%$, taking into account the gauge factor of constantan $G=2(\Delta L/L \approx G^{-1}\Delta R/R)$. This length change along the a axis corresponds well that obtained by x-ray diffraction on $CaFe_2As_2$.[14] On the other hand, for measurements in phase II, where the freezing temperature of the pressure medium exceeds T_S, the length change becomes distributed over a very broad temperature range below the onset of the transition, which implies a wide range of coexisting paramagnetic phase and antiferromagnetic orthorhombic phase. This also is consistent with a microscopic probe of the structure by NMR.[38]

We interpret our observations as follows: at the phase I/phase II boundary, domains of cT phase begin to nucleate in the matrix of magnetic O domains, and the relative fraction of these domains reverses as the phase II/phase III boundary is approached. Though scattering at domain walls could account, in part, for the higher ρ_0 in phase II relative to phase III, the density of domain walls would need to be nonmonotonic as a function of pressure to account for a maximum in ρ_0 shown in Fig. 4(a). This seems unlikely. Alternatively, increased scattering in phase II by dynamical processes provides a more plausible interpretation. The qualitatively lower resistivity over a broad temperature range in the pure cT phase implies a higher density of charge carriers than in the O structure, contrary to naive expectations from band structure calculations that find a reduced density of states in the cT structure.[39] These "doped" carriers from the cT phase are scattered by fluctuations associated with the O structure. The origin of these fluctuations could be twofold. In a strong coupling, local-moment picture of the magnetism, magnetic fluctuations are expected as the spin structure of O domains becomes increasingly frustrated due to a pressure-induced increase in As-As and Fe-As hybridization at pressures above 0.3 GPa.[40,41] On the other hand, in a weak coupling, spin-density-wave (SDW) model, these changes in hybridization also will modify details of Fermi-surface topology and nesting conditions for the SDW, leading to spin fluctuations from nearly nested parts of the Fermi surface.[42] The correlation between an increase in ρ_0 and T_c as well as the maximum in $-\Delta\chi_{ac}$ in phase II is a consequence of the pressure dependence of the volume fraction of O and cT, where the O phase is the necessary source of magnetic fluctuations and the cT phase the source of carriers. The coupled spin-"doped" charge dynamics and bulk superconductivity,

present only because of structural inhomogeneity, are absent in pure O and cT structures. Whether or not the domain structure is static or dynamic in phase II cannot be established from these experiments, but expected pressure gradients at O/cT domain walls, due to significant structural differences of the phases,[21] could favor temporal fluctuations of the domains and Fe moments of the O structure.[43] Without a small pressure inhomogeneity inevitable with a soft but frozen pressure medium, it is not possible to nucleate the structural inhomogeneity that induces internal strain, which in turn stabilizes the composite structural phases.

The cT phase depends strongly on pressure history, as shown in Fig. 4(b). Decreasing pressure from highest pressures locks in the low residual resistivity of phase III to a pressure much below 0.8 GPa; there is no maximum in ρ_0 for $0.3 \leq P \leq 0.8$ GPa, and the maximum in $-\Delta\chi_{ac}$ appears near 0.3 GPa, all in contrast to results on increasing pressure. Recovery of the initial residual resistivity at ambient pressure suggests that the orthorhombic structure is the stable low-temperature structure upon decreasing pressure, as concluded as well in recent structural studies.[37] These conclusions also are consistent with the pressure dependence of T_S determined on decreasing pressure [Fig. 2(b)]. The strong pressure hysteresis of the boundary between phases II and III and large thermal hysteresis at T_S^h will induce structural and electronic inhomogeneities on decreasing pressure and further complicate an interpretation of $T_c(P)$ with decreasing pressure.

In summary, pressure-dependent resistivity and ac susceptibility measurements reveal strong coupling among superconductivity, structure, and magnetism in $CaFe_2As_2$. The coexisting phase, which exists in a narrow window of increasing pressure, supports bulk superconductivity due to the coupled spin-charge dynamics special to the coexistence.

Work at Los Alamos was performed under the auspices of the U.S. Department of Energy/Office of Science and supported by the Los Alamos LDRD program. T.P. acknowledges support from KOSEF (Grant No. 2009-0058687) funded by the Korea government (MEST). V.A.S. acknowledges support from the Russian Foundation for Basic Research (Grant No. 09-02-00336).

[1] Y. Kamihara, T. Watanabe, M. Hirano, and H. Hosono, J. Am. Chem. Soc. **130**, 3296 (2008).
[2] X. H. Chen, T. Wu, G. Wu, R. H. Liu, H. Chen, and D. F. Fang, Nature (London) **453**, 761 (2008).
[3] Z.-A. Ren, Jie Yang, Wei Lu, Wei Yi, Xiao-Li Shen, Zheng-Cai Li, Guang-Can Che, Xiao-Li Dong, Li-Ling Sun, Fang Zhou, and Zhong-Xian Zhao, EPL **82**, 57002 (2008).
[4] Z.-A. Ren, J. Yang, W. Lu, W. Yi, G. C. Che, X. L. Dong, L. L. Sun, and Z. X. Zhao, Mater. Res. Innovations **12**, 105 (2008).
[5] R. H. Liu, G. Wu, T. Wu, D. F. Fang, H. Chen, S. Y. Li, K. Liu, Y. L. Xie, X. F. Wang, R. L. Yang, L. Ding, C. He, D. L. Feng, and X. H. Chen, Phys. Rev. Lett. **101**, 087001 (2008).
[6] I. I. Mazin, D. J. Singh, M. D. Johannes, and M. H. Du, Phys. Rev. Lett. **101**, 057003 (2008).
[7] M. Rotter, M. Tegel, D. Johrendt, I. Schellenberg, W. Hermes, and R. Pottgen, Phys. Rev. B **78**, 020503(R) (2008).
[8] N. Ni, S. L. Budko, A. Kreyssig, S. Nandi, G. E. Rustan, A. I. Goldman, S. Gupta, J. D. Corbett, A. Kracher, and P. C. Canfield, Phys. Rev. B **78**, 014507 (2008).
[9] J.-Q. Yan, A. Kreyssig, S. Nandi, N. Ni, S. L. Bud'ko, A. Kracher, R. J. McQueeney, R. W. McCallum, T. A. Lograsso, A. I. Goldman, and P. C. Canfield, Phys. Rev. B **78**, 024516 (2008).
[10] C. Krellner, N. Caroca-Canales, A. Jesche, H. Rosner, A. Ormeci, and C. Geibel, Phys. Rev. B **78**, 100504(R) (2008).
[11] G. F. Chen, Li Zheng, Li Gang, Hu Wan-Zheng, Dong Jing, Zhou Jun, Zhang Xiao-Dong, Zheng Ping, Wang Nan-Lin, and Luo Jian-Lin, Chin. Phys. Lett. **25**, 3403 (2008).
[12] F. Ronning, T. Klimczuk, E. D. Bauer, and J. D. Thompson, J. Phys.: Condens. Matter **20**, 322201 (2008).
[13] G. Wu, H. Chen, T. Wu, Y. L. Xie, Y. J. Yan, R. H. Liu, X. F. Wang, J. J. Ying, and X. H. Chen, J. Phys.: Condens. Matter **20**, 422201 (2008).
[14] N. Ni, S. Nandi, A. Kreyssig, A. I. Goldman, E. D. Mun, S. L. Bud'ko, and P. C. Canfield, Phys. Rev. B **78**, 014523 (2008).
[15] M. Rotter, M. Tegel, and D. Johrendt, Phys. Rev. Lett. **101**, 107006 (2008).
[16] A. S. Sefat, R. Jin, M. A. McGuire, B. C. Sales, D. J. Singh, and D. Mandrus, Phys. Rev. Lett. **101**, 117004 (2008).
[17] T. Park, E. Park, H. Lee, T. Klimczuk, E. D. Bauer, F. Ronning, and J. D. Thompson, J. Phys.: Condens. Matter **20**, 322204 (2008).
[18] M. S. Torikachvili, S. L. Bud'ko, N. Ni, and P. C. Canfield, Phys. Rev. Lett. **101**, 057006 (2008).
[19] P. L. Alireza, Y. T. Chris Ko, J. Gillett, C. M. Petrone, J. M. Cole, G. G. Lonzarich, and S. E. Sebastian, J. Phys.: Condens. Matter **21**, 012208 (2009).
[20] A. I. Goldman, D. N. Argyriou, B. Ouladdiaf, T. Chatterji, A. Kreyssig, S. Nandi, N. Ni, S. L. Budko, P. C. Canfield, and R. J. McQueeney, Phys. Rev. B **78**, 100506(R) (2008).
[21] A. Kreyssig, M. A. Green, Y. Lee, G. D. Samolyuk, P. Zajdel, J. W. Lynn, S. L. Bud'ko, M. S. Torikachvili, N. Ni, S. Nandi, J. B. Leão, S. J. Poulton, D. N. Argyriou, B. N. Harmon, R. J. McQueeney, P. C. Canfield, and A. I. Goldman, Phys. Rev. B **78**, 184517 (2008).
[22] T. Goko, A. Aczel, E. Baggiosaitovitch, S. Budko, P. Canfield, J. Carlo, G. Chen, P. Dai, A. Hamann, W. Hu, H. Kageyama, G. Luke, J. Luo, B. Nachumi, N. Ni, D. Reznik, D. Sanchezcandela, A. Savici, K. Sikes, N. Wang, C. Wiebe, T. Williams, T. Yamamoto, W. Yu, and Y. Uemura, arXiv:0808.1425 (unpublished).
[23] W. Yu, A. A. Aczel, T. J. Williams, S. L. Bud'ko, N. Ni, P. C. Canfield, and G. M. Luke, Phys. Rev. B **79**, 020511(R) (2009).
[24] M. Kumar, M. Nicklas, A. Jesche, N. Caroca-Canales, M. Schmitt, M. Hanfland, D. Kasinathan, U. Schwarz, H. Rosner, and C. Geibel, Phys. Rev. B **78**, 184516 (2008).
[25] H. Kotegawa, H. Sugawara, and H. Tou, J. Phys. Soc. Jpn. **78**, 013709 (2009).
[26] K. Igawa, Hironari Okada, Hiroki Takahashi, Satoru Matsuishi,

Yoichi Kamihara, Masahiro Hirano, Hideo Hosono, Kazuyuki Matsubayashi, and Yoshiya Uwatoko, J. Phys. Soc. Jpn. **78**, 025001 (2009).
[27] H. Fukazawa, Nao Takeshita, Takehiro Yamazaki, Kenji Kondo, Kenji Hirayama, Yoh Kohori, Kiichi Miyazawa, Hijiri Kito, Hiroshi Eisaki, and Akira Iyo, J. Phys. Soc. Jpn. **77**, 105004 (2008).
[28] A. Mani, N. Ghosh, S. Paulraj, A. Bharathi, and C. S. Sundar, arXiv:0903.4236 (unpublished).
[29] A. Eiling and J. S. Schilling, J. Phys. F: Met. Phys. **11**, 623 (1981).
[30] S. Klotz, J.-C. Chervin, P. Munch, and G. Le Marchand, J. Phys. D **42**, 075413 (2009).
[31] V. A. Sidorov (unpublished).
[32] S.-H. Baek, N. J. Curro, T. Klimczuk, E. D. Bauer, F. Ronning, and J. D. Thompson, Phys. Rev. B **79**, 052504 (2009).
[33] N. Kumar, R. Nagalakshmi, R. Kulkarni, P. L. Paulose, A. K. Nigam, S. K. Dhar, and A. Thamizhavel, Phys. Rev. B **79**, 012504 (2009).
[34] A. A. Aczel, E. Baggio-Saitovitch, S. L. Budko, P. C. Canfield, J. P. Carlo, G. F. Chen, Pengcheng Dai, T. Goko, W. Z. Hu, G. M. Luke, J. L. Luo, N. Ni, D. R. Sanchez-Candela, F. F. Tafti, N. L. Wang, T. J. Williams, W. Yu, and Y. J. Uemura, Phys. Rev. B **78**, 214503 (2008).
[35] S. Takeshita and R. Kadono, New J. Phys. **11**, 035006 (2009).
[36] Y. J. Uemura, A. Keren, L. P. Le, G. M. Luke, B. J. Sternlieb, W. D. Wu, J. H. Brewer, R. L. Whetten, S. M. Huang, Sophia Lin, R. B. Kaner, F. Diederich, S. Donovan, G. Grüner, and K. Holczer, Nature (London) **352**, 605 (1991).
[37] A. I. Goldman, A. Kreyssig, K. Prokeš, D. K. Pratt, D. N. Argyriou, J. W. Lynn, S. Nandi, S. A. J. Kimber, Y. Chen, Y. B. Lee, G. Samolyuk, J. B. Leão, S. J. Poulton, S. L. Bud'ko, N. Ni, P. C. Canfield, B. N. Harmon, and R. J. McQueeney, Phys. Rev. B **79**, 024513 (2009).
[38] S.-H. Baek, H. Lee, S. E. Brown, N. J. Curro, E. D. Bauer, F. Ronning, T. Park, and J. D. Thompson, Phys. Rev. Lett. **102**, 227601 (2009).
[39] T. Yildirim, Phys. Rev. Lett. **102**, 037003 (2009).
[40] T. Yildirim, Phys. Rev. Lett. **101**, 057010 (2008).
[41] M. J. Han, Q. Yin, W. E. Pickett, and S. Y. Savrasov, Phys. Rev. Lett. **102**, 107003 (2009).
[42] For example, V. Stanev, J. Kang, and Z. Tesanovic, Phys. Rev. B **78**, 184509 (2008).
[43] I. I. Mazin and M. D. Johannes, Nat. Phys. **5**, 141 (2009).